PHF6-altered T-ALL harbored epigenetic repressive switch at bivalent promoters and respond to 5-azacitidine and venetoclax

Antoine Pinton, Lucien Courtois, Charlotte Doublet, Aurélie Cabannes-Hamy, Guillaume Andrieu, Charlotte Smith, Estelle Balducci, Agata Cieslak, Aurore Touzart, Mathieu Simonin, et al.

PHF6-altered T-ALL harbored epigenetic repressive switch at bivalent promoters and respond to 5-azacitidine and venetoclax

Antoine Pinton[1], Lucien Courtois[1], Charlotte Doublet[2], Aurélie Cabannes-Hamy[3], Guillaume Andrieu[1], Charlotte Smith[1], Estelle Balducci[1], Agata Cieslak[1], Aurore Touzart[1], Mathieu Simonin[1], Véronique Lhéritier[4], Françoise Huguet[5], Marie Balsat[6], Hervé Dombret[7,8], Philippe Rousselot[3], Salvatore Spicuglia[10,11], Elizabeth Macintyre[1], Nicolas Boissel[7,8], Vahid Asnafi[1].

Affiliations :

1- Institut Necker Enfants-Malades, INSERM U1151. Hôpital Necker Enfants-Malades, Laboratoire d'Onco-Hématologie, Assistance Publique – Hôpitaux de Paris, and université Paris-Cité, Paris, France
2- Centre Hospitalier Annecy Genevois, Epagny Metz-Tessy, France
3- Centre Hospitalier de Versailles, Versailles, France
4- Coordination du Groupe Group for Research in Adult Acute Lymphoblastic Leukemia, Hospices Civils de Lyon, Hôpital Lyon Sud, Lyon, France.
5- Service d'Hématologie, CHU de Toulouse, IUCT-Oncopole, Toulouse, France.
6- Service d'hématologie clinique, Hôpital Lyon Sud, Lyon, France.
7- Service d'Hématologie Adolescents et Jeunes Adultes, Hôpital Saint-Louis, Assistance Publique-Hôpitaux de Paris, Paris, France
8- Institut de Recherche Saint-Louis, UPR-3518, Université Paris Cité, Paris, France.
9- Université Versailles St Quentin en Yvelines Paris Saclay, INSERM U1184
10- Aix-Marseille University, Inserm, TAGC, UMR1090, Marseille, France.
11- Equipe Labélisée Ligue Contre le Cancer, Marseille, France.

Running title :
PHF6^{ALT} T-ALL respond to 5-azacitidine and venetoclax

Corresponding author :
Hôpital Necker-Enfants Malades - Laboratoire d'Onco-hématologie
149 rue de Sèvres 75015 Paris
Telephone : +33 1 44 49 49 14
Email : vahid.asnafi@nck.aphp.fr

Conflicts of interest :
The authors have declared that no conflict of interest exists.

Abstract

Purpose: To assess the impact of PHF6 alterations on clinical outcome and therapeutical actionability in T cells acute lymphoblastic leukemia (T-ALL).

Experimental Design: We described PHF6 alterations in an adult cohort of T-ALL from the French trial GRAALL 2003/2005 and retrospectively analyzed clinical outcomes between PHF6-altered ($PHF6^{ALT}$) and wild-type patients. We also used EPIC and ChIP-seq data of patient samples to analyze the epigenetic landscape of $PHF6^{ALT}$ T-ALLs. We consecutively evaluated 5-azacitidine efficacy, alone or combine with venetoclax, in $PHF6^{ALT}$ T-ALL.

Results: We show that PHF6 alterations account for 47% of cases in our cohort and demonstrate that $PHF6^{ALT}$ T-ALL presented significantly better clinical outcomes. Integrative analysis of DNA methylation and histone marks shows that $PHF6^{ALT}$ are characterized by DNA hypermethylation and H3K27me3 loss at promoters physiologically bivalent in thymocytes. Using patient-derived xenografts (PDX), we show that $PHF6^{ALT}$ T-ALL respond to the 5-azacytidine alone. Finally, synergism with the BCL2-inhibitor venetoclax was demonstrated in refractory/relapsing $PHF6^{ALT}$ T-ALL using fresh samples. Importantly, we report three cases of refractory/relapsed (R/R) $PHF6^{ALT}$ patients who were successfully treated with this combination.

Conclusions: Overall, our study supports the use of PHF6 alterations as a biomarker of sensitivity to 5-azacytidine and venetoclax combination in R/R T-ALL.

Translational Relevance

Predicting and treating R/R T-ALL remains a major challenge and require improved patient prognosis stratification and biomarkers for targeted therapies. PHF6 is frequently mutated in adult T-ALL, but the impact of its alterations on clinical outcome and their actionability as a therapeutic target remain elusive. We describe PHF6 alterations in 216 T-ALL and show that PHF6 loss of function is associated with better outcome, independently of other known prognostic parameters. Using multiomics approaches, we demonstrate that PHF6 alterations in T-ALL is associated with DNA hypermethylation and H3K27me3 loss at promoters physiologically bivalent in thymocytes. Using fresh samples of R/R T-ALL, we revealed increased in vivo sensitivity of $PHF6^{ALT}$ T-ALL to the demethylating agent 5-azacitidine alone or associated with the BCL2-inhibitor venetoclax. We report three cases of R/R $PHF6^{ALT}$ T-ALL patients successfully treated with this combination. Overall, our study supports the use of PHF6 alterations as a biomarker of eligibility to 5-azacytidine and venetoclax in R/R T-ALL.

Introduction

T-cell acute lymphoblastic leukemia (T-ALL) is a heterogeneous hematological disease resulting from malignant proliferation of immature thymic cell precursors blocked at varying stages of differentiation, which partially recapitulates normal lymphoid T-cell ontogeny (1). T-ALL mostly occurs in children and young adults (10%-15% and 20%-25% of ALL cases, respectively) (2). The use of intensive chemotherapy regimens has considerably improved the outcome of adult T-ALL. Yet, refractory and relapsed disease conveys a dismal prognosis with a 6-to-9 months median survival (2–5). Therefore, improving patient prognosis stratification and finding biomarkers for innovative targeted therapies is of major importance. Epigenetic alterations are frequent events in T-ALL and can offer unique therapeutic vulnerabilities to epigenetic modifiers such as the hypomethylating agent 5-azacytidine. However, the eligibility of T-ALL patients to this therapy is still debated (6,7).

Plant Homeodomain Finger protein 6 gene (*PHF6*) was originally identified as the causative gene of Börjesson-Forsmann-Lehman syndrome (BFLS), a rare X-linked neurodevelopmental disorder (8). *PHF6* is frequently altered by somatic LoF mutations and deletions in T-ALL (~40% adult and ~15% pediatric cases) and T/M mixed-phenotype acute leukemia (MPAL), and less frequently in myeloid malignancies or clonal hematopoïesis (9–14). The PHF6 protein localizes within the nucleolus where it support a role in the control of transcription and ribosome biogenesis (15,16). In addition, PHF6 has been demonstrated to control chromatin accessibility through interaction with chromatin remodelers such as NuRD and SWI/SNF complexes (15,17–19).

PHF6 alterations are associated with NOTCH1 and IL7R/JAK/STAT pathway genes gain-of-function mutations, PRC2 complex genes LoF mutations, *WT1* and *PTPN2*

deletions and TLX1 or TLX3 ectopic expression (20–27). Analysis of clonal evolution and mutation dynamics using paired diagnostic and relapse samples identified PHF6 LoF as an early events in T leukemogenesis (28). Mechanistically, increased self-renewal in the hematopoietic stem cell compartment following *PHF6* LoF have been reported as a major feature contributing to leukemia (28–31). Even though *PHF6* alterations are often found in adult T-ALL, their impact on prognosis and their therapeutic actionability remain poorly explored (31–33).

In this study, we analyzed *PHF6* alterations in a large cohort of adult T-ALL from the Group for Research on Adult Acute Lymphoblastic Leukemia (GRAALL) 03/05 French trials. Our data demonstrate that *PHF6* alterations in T-ALL lead to DNA hypermethylation and is associated with response to demethylating drugs alone or in combination with the BCL2 inhibitor venetoclax.

Material and Methods

Patients enrolled in the GRAALL 2003-2005 study

Patients were enrolled in the GRAALL-2003-2005 trials (registered on http://clinicaltrials.gov as follows: GRAALL-2003, #NCT00222027; GRAALL-2005, #NCT00327678). 216 patients out of 337 were included in this study based on DNA availability for molecular analyses. No differences in clinical outcomes were observed between the included patients and the entire cohort (data not shown). Diagnostic samples were collected after informed consent according to the Declaration of Helsinki. Immunophenotyping was performed as previously described (1). All samples used contained at least 80% blasts. Patient minimal residual disease (MRD) was assessed as previously described (59).

Patients enrolled in the ALL-TARGET study

The three 5-AZA-Venetoclax treated-patients reported in this manucript have been registred within the ALL-TARGET, Registry of Relapsed/Refractory T-cell Acute Lymphoblastic Leukemia, trial. This study has been registered on ClinicalTrials.gov. under NCT05832125 references.

Next-generation sequencing, copy number, and molecular analyses

Genomic analysis was performed by pan-exon targeted next-generation sequencing of DNA extracted from diagnosis samples. The next-generation sequencing panel included 103 genes relevant in hematological malignancies (Nextera XT gene panel; Illumina, San Diego, CA). Libraries were prepared according to Illumina instructions and sequenced on a MiSeq instrument (Illumina; 500× with mean coverage 95%). Sequence reads were aligned to the reference genome (GRCh38) using our in-house software Polyweb (Institut Imagine, Paris). Variant filtering and calling were performed using validated criteria (coverage <30×, <10 alternative reads or variant allelic fraction < 7%, polymorphisms described in dbSNP, 1000Genomes, EVS, Gnomad, and EXAC with a calculated mean population frequency >0.1%); annotations were done using somatic database COSMIC and ProteinPaint (St Jude Children's Research Hospital—Pediatric Cancer data portal). Some mutations were confirmed by Sanger sequencing. Copy number variants were assessed either by multiplex ligation-dependent probe amplification technique (SALSA-multiplex ligation-dependent probe amplification P383 T-ALL probe mix (MRC-Holland, Amsterdam, Netherlands) kit containing 53 probes for 13 different chromosomic regions of diagnostic or prognostic importance in T-ALL. PHF6 deletions were confirmed by high-resolution array comparative genomic hybridization as previously reported (35).

EPIC array analysis

Intensity Data (IDAT) files from Illumina Infinium Methylation EPIC BeadChip (EPIC arrays) were processed and normalized with RnBeads Bioconductor package. Probes with high SNP probability and bad detection P-values were filtered out. EPIC arrays were also used for copy number analysis using the conumee Bioconductor package, and further processed with GISTIC2 to identify recurrent copy number aberrations. Probes located in regions with altered copy numbers were excluded from downstream analysis. Differential methylation analysis was performed using Limma R package (60).

ChIP-seq analysis

BAM files for thymocytes ChIP-seq datasets were obtained from the BLUEPRINT consortium. Peak calling was performed as previously described (38). Regulatory features were found by overlapping histone marks peaks with the GenomicRanges R package. Enrichment analysis of DMPs within regulatory regions was performed with the LOLA Bioconductor package. As background probes, we used all the annotated probes of the EPIC analysis.

RNA sequencing and data analysis

For T-ALL, 89 primary samples with eligible RNA were analyzed by poly(A)-enriched RNA-Seq. Fragments were sequenced in stranded paired-end mode (2×50 bp) using the Agilent platform. Variance-stabilized log2 expression values were computed using DESEq2 R package. Z-scores of log2 expression values were computed to perform hierarchical clustering analysis using Euclidean distance and complete clustering method arguments with ComplexHeatmap R package. Uniform Manifold Approximation and Projection for dimension reduction was performed using the M3C R package.

Patient-derived xenografts

Patient-derived xenografts (PDX) were generated from primary T-ALL samples as previously reported.38 106 viable leukemic cells were xenografted by intravenous retro-orbital injection in 6-weeks old NSG mice. Mice were monitored weekly by flow cytometry for leukemic load (FSChi, hCD7+, hCD45+ cells) in peripheral blood. Animal were clinically and biologically monitored until endpoint was reached or terminally ill, according to local ethical rules and home office license (30078-2021021814199445). Bone marrows from tibiae, hip, femora and vertebrae were collected for subsequent ex vivo experiments. All samples used contained ≥90% blasts.

PDX 5-azacytidine treatment

Mice were treated in a “curative-like” setting, starting when peripheral blood blast counts exceeded 1%. They received 5 mg/kg/day 5-Azacytidine intra-peritoneally (IP) for five days twice with two days break. Untreated mice received the same volume of NaCl IP. Mice were sacrificed when the blast fraction was more than 80% or if mice presented clinical signs of disease (loss of weight >10%, neurological symptoms, tumor development). The national ethics committee approved the mouse study: PROJET APAFIS # 8853 N° 2017020814103710.

Cytotoxic assay of fresh patient samples

Fresh blast-infiltrated samples were counted for cellularity, assayed by flow cytometry to quantify blast-infiltration. Samples had at least 20.10^6 cells with more than 25% blasts and 50% of viability before incubation with drugs. Cell suspension was incubated with 1.25 to 5 µg/µL of 5-azacytidine combined, or not with 125 µM of venetoclax. Cells were then cultured in a complete medium supplemented with cytokines, at 37°C. After 3 days of incubation, cell viability was assessed by flow cytometry (Annexin-V/Propidium iodide).

Statistical analyses

Statistical analyses were performed using GraphPad Prism 8 software and R (version 4.2.0). The following were used to indicate significant differences: • : P > 0.05; * : P < 0.05; ** : P < 0.01; *** : P <0 .001; **** : P <0 .0001.

Data availability

The data generated in this study are not publicly available due to information that could compromise patient privacy or consent but are available upon reasonable request from the corresponding author, vahid.asnafi@aphp.fr.

Results

PHF6 alterations are frequent in adult T-ALL

To assess the prevalence of *PHF6* alterations in T-ALL, we analyzed data from targeted whole-exome sequencing and copy number analysis previously obtained for 216 adult patients from the GRAALL-03/05 protocols (34). 47% patients had at least one *PHF6* LoF alteration in our cohort (102 ALT patients versus 114 WT) (Figure 1A). The most frequent alterations were nonsense mutations followed by frameshift indels and missense mutations (Figure 1B-C). Truncating mutations were frequently located within the 5' half of the protein whereas missense mutations were almost exclusively found at the ePHD2 and 3' PHD zinc finger domain.

We then compared the oncogenetic landscape between $PHF6^{ALT}$ and $PHF6^{WT}$ T-ALL *PHF6* LoF was significantly associated with increased mutational rates of *WT1* and *RUNX1*, and decreased mutational rate of *ETV6*, three transcription factors known to be frequently altered in immature T-ALL. As previously reported, *PHF6* alterations frequently co-occurred with activating NOTCH1 and IL7R pathway (*IL7R*, *JAK1*, *JAK3*, *STAT5B*, *DNM2*, *PTPRC*, *PTPN2*) mutations. The RAS signaling regulator NF1 was

also frequently co-inactivated. Among epigenetic factors, *PHF6* alterations were associated with increased mutational rates of the PRC2 complex gene *SUZ12*, *ASXL1* and *CTCF*. Conversely, *PHF6* alterations segregated from mutations in *DNMT3A* and *IDH2*, both implicated in DNA methylation process (Figure 1D-E and Supplementary Figure S1A). *PHF6* alterations were less frequent in mature TCRAB expressing T-ALL (25% vs 75% with p = 0.01) (Figure 1F). Consistent with seminal studies, *PHF6* LoF anomalies were significantly associated with ectopic expression of both TLX1 and TLX3 with marked enrichment in the TLX1 subtype (35% vs 12% with p < 1.10-4 and 19% vs 9% with p = 0.03 respectively) (Figure 1G). In line with their absence in TCRAB expressing T-ALL, *PHF6* alterations were virtually absent from the TAL1 deregulated subtype (1% in *PHF6*^{ALT} T-ALL vs 26% in *PHF6*^{WT} cases, p < 1.10-4).

Finally, we addressed the question of the conservation of *PHF6* alterations from diagnosis to relapse. In a series of 5 protocolar paired diagnosis/relapsed *PHF6*^{ALT} patients, all retained *PHF6* alteration at relapse (Supplementary Figure S1B). We decided to confirm these results on a larger non protocolar cohort of 37 other patients bearing PHF6 pathogenic variant at diagnosis (Supplementary Table 1). Among them, 35 (95%) retained PHF6 alteration at relapse. These results suggest that *PHF6* alterations are strongly conserved during the clonal evolution of the disease.

PHF6 alterations are associated with better clinical outcomes in the GRAALL-03/05 protocols

A clinical and biological comparison of cases with and without *PHF6* alterations is shown in Table 1. *PHF6*^{ALT} patients were significantly older than the rest of the cohort (median age of 34.17 versus 28.22 years with p = 0.04).

We also analyzed treatment response in *PHF6*^{ALT} and *PHF6*^{WT} cases in our cohort. There was no significant difference between the two groups regarding steroid response and early bone marrow blast clearance. Nevertheless, and despite older age, *PHF6*^{ALT} patients had significantly lower rates of death during induction (1% versus 7%, p = 0.04), and higher attainment of complete remission (96% versus 89%, p = 0.05). Mutated patients had better outcomes at five years estimation in terms of overall survival, event-free survival, and cumulative incidence of relapse.

By univariate analysis, *PHF6*^{ALT} patients had significantly increased overall survival (HR 0.51, p = 0.004)(Table 1 and Figure 2). This benefit remained significant by multivariate analysis and was independent from the High risk genetic classifier (HR of 0.58 with p = 0.03) (35). Overall, our results show that *PHF6* LoF mutations are associated with better treatment response and survival and should be considered when assessing patient prognosis.

PHF6^{ALT} T-ALL display DNA hypermethylation at promoters of physiological PRC2 target genes

PHF6 being a known epigenetic modulator, we sought to explore the epigenetic landscape of *PHF6*^{ALT} T-ALL. We thus performed genome-wide methylation analysis, taking advantage of data formerly generated by our team, in a series of 143 primary adult T-ALL samples (7). Genome-wide DNA methylation was significantly higher in

PHF6^{ALT} when compared to WT patients (Figure 3A). These results are coherent with our previous paper on DNA methylation in T-ALL in which PHF6 alterations seemed to be associated with hypermethylated cluster C3, C4 and C5 (7). Indeed PHF6 alterations were significantly enriched in clusters C3 and C4 (15/22, $p = 0.01$ and 30/41, $p < 0.001$ respectively) and almost absent from C1 and C2 hypomethylated clusters (0/14, $p < 0.001$ and 1/34, $p < 0.001$ respectively)(Supplementary Figure S2A). There was no significant enrichment for PHF6 alterations in cluster C5 (16/32, $p = 0.25$). This cluster was reported to have dismal outcomes in our previous paper. We thus checked if PHF6 status could refine the overall survival prognosis in this cluster. Interestingly yet not significantly, PHF6^{ALT} patients from the C5 cluster had a tendency towards better overall survival than their WT counterpart (Supplementary Figure S2B).

Differential methylation analysis identified a total of 42,164 differentially methylated probes (DMP) (39,286 hypermethylated and only 2,878 hypomethylated DMP) in *PHF6*^{ALT} T-ALL when compared to *PHF6*^{WT} (Figure 3B). Hypermethylated DMPs (hyDMPs) were strongly enriched in CpG islands (CGIs), regardless of their genomic location. Hypomethylated DMPs were enriched in CpG open seas and shores and preferentially located at distal regions of promoter and gene body (Figure 3C and 4D). Of note, hyDMPs were strictly hypomethylated in normal thymocytes (Figure 3E). A total of 3,066 protein-coding gene-associated promoters were hypermethylated and 431 were hypomethylated in *PHF6*^{ALT} T-ALL (Figure 3F). Hypermethylated promoters were associated with H3K27me3 and H3K4me3 histone marks in CD34+ and CD3+ cells (Figure 3G). ChIP-seq analysis of these promoters at different stages of normal thymocytes revealed simultaneous H3K4me3 and H3K27me3 marks, representing bivalent chromatin domains, a hallmark of developmentally regulated genes (Figure 3H) (36,37). Consistently, these promoters were enriched in target genes of SUZ12

and EZH2, two subunits of the PRC2 complex, responsible for H3K27me3 histone mark deposition and a major regulator of bivalent chromatin.

PHF6 and *SUZ12* alterations significantly co-occur in our cohorts, therefore, to prevent potential confounding factors, patients were separated into *PHF6* altered only, PRC2 altered only (with alterations of *SUZ12*, *EED* or *EZH2*), both altered, or none altered. T-ALL bearing alterations in either *PHF6*, PRC2 or in both, had significantly higher overall DNA methylation (Figure 3I). These T-ALL shared 30,839 hyDMPs when compared to T-ALL with no alterations and constitute a coherent cluster on UMAP projection of methylome profile (Figure 3J and K). These hyDMPs were also enriched at genes associated with H3K27me3 and H3K4me3 histone marks in CD34+ and CD3+ cells and affiliated with gene ontology terms related to developmental processes, transcription regulation, cell proliferation and central nervous system differentiation (Figure 3L). Altogether, our data suggest that *PHF6*^{ALT} T-ALL display DNA hypermethylation at promoters of physiological PRC2 target genes.

PHF6^{ALT} T-ALL display altered epigenetics landscape of bivalent promoters with loss of H3K27me3 and DNA hypermethylation

Given the enrichment of hyDMPs in both H3K27me3 and H3K4me1/3, we hypothesized that *PHF6*^{ALT} T-ALL display aberrant DNA hypermethylation and profound alteration of bivalent promoters.

We therefore performed enrichment analysis for regulatory elements on hyDMPs using ChIP-seq data of H3K4me3 and H3K27me3 histone marks. Two types of promoters were defined and studied (active and bivalent) (38). To assess the possible implication of major oncotypes we also studied the distribution of TLX1, TAL1 and PHF6 binding sites by using publicly available ChIP-seq data (39). hyDMPs and PHF6-bound regions

were strikingly enriched in bivalent promoters. Of note, among known genes targeted by PHF6 (118 genes), 11 (~10%) are also found in repressed bivalent genes (Supplementary Table 2). Genomic regions bound by TAL1 or TLX1 did not overlap with bivalent promoters but exclusively with active one (Figure 4A). Unsupervised hierarchical clustering of DNA methylation level efficiently segregated samples according to their oncotype when considering active promoters, while bivalent ones separated *PHF6*^{ALT} T-ALL from *PHF6*^{WT} T-ALL and normal thymocytes, regardless of the oncotype (Figure 4B). Strikingly, a subset of *PHF6*^{WT} T-ALL, strongly enriched in TAL1 oncotype showed very similar methylation profile of bivalent promoters to normal thymocytes, with very low levels of DNA methylation. UMAP projection according to bivalent promoters methylation levels displayed similar results (Figure 4C). Hypermethylation of bivalent regions has already been described and usually follows the loss of bivalent histone marks (40–42). To look for epigenetic changes in histone mark deposition following *PHF6* LoF, we analyzed H3K27me3 and H3K4me3 ChIP-seq peaks from 8 T-ALL (4 *PHF6*^{WT}/ PRC2^{WT}, 2 *PHF6*^{ALT}, PRC2^{ALT}, *PHF6*^{ALT}/ PRC2^{ALT}) at thymic bivalent promoters. *PHF6*^{ALT} T-ALL had a profound reduction of H3K27me3 peaks at thymic bivalent promoters when compared with WT T-ALL (Figure 4D). Among the 2278 thymic bivalent genes, 1545 were associated to hyDMPs (Figure 4E). Surprisingly, PRC2^{ALT} T-ALL had no reduction of H3K27me3 peaks while *PHF6*^{ALT}/ PRC2^{ALT} had profiles similar to *PHF6*^{ALT}. The analysis of H3K4me3 marks gave comparable results, although less pronounced. These results suggest a role for PHF6 in the maintenance of H3K27me3 histone mark and of low levels of DNA methylation at bivalent promoters.

We then sought to assess hyDMRs-associated bivalent gene expression in T-ALL and look for differential expression between *PHF6*^{ALT} and *PHF6*^{WT} samples. We therefore

performed differential expression analysis using bulk RNA-seq on 89/216 primary clinical samples (49 WT and 40 ALT). Out of the 1548 bivalent genes associated with hyDMRs, only 65 were differentially expressed between the two conditions (27 upregulated and 38 downregulated in *PHF6*^{ALT} T-ALL), suggesting epigenetic alteration of bivalent promoter has minimal impact on bivalent genes expression at the stage of patent leukemia (Figure 4F).

PHF6^{ALT} T-ALL are sensitive to hypomethylating agents alone or in combination with BCL2 inhibitor venetoclax

PHF6^{ALT} T-ALL have significantly higher level of global DNA methylation. We thus reasoned that treatment with hypomethylating agents could be of potential interest in the treatment of these T-ALL. To first confirm this rational, we took advantage of results previously generated with patient derived xenografts (PDX) from 4 primary T-ALL samples (2 *PHF6* WT (UPNT-M525 / UPNT-M894) and 3 ALT (UPNT-M149 / UPNT-670)) (7). Treatment was initiated when peripheral blood (PB) blast counts exceeded 1%. Mice were given 5-azacytidine in vivo or left untreated. For PDX derived from *PHF6*^{ALT} patients, curative 5-azacytidine treatment significantly increased survival (Figure 5A). There were no differences in terms of survival between treated and untreated mice derived from *PHF6*^{WT} patients-derived PDX. These results suggest that *PHF6*^{ALT} T-ALL indeed display increased vulnerability to demethylating agents.

R/R disease being a major problem in T-ALL, due to particularly poor prognosis, we examined whether 5-azacytidine could be used to treat patients at relapse. We therefore performed ex vivo cytotoxic assays using 5-azacytidine on fresh blasts infiltrated samples from 21 R/R T-ALL patients collected within the French ALL-Target protocol (9 *PHF6*^{ALT}, 5 PRC2^{ALT}, 7 WT)(Supplementary Table 3). *PHF6*^{ALT} samples had significantly better response to 5-azacytidine than WT (Figure 5B). Coherently with

their comparable DNA methylation profile, similar results could be observed for PRC2^{ALT} T-ALL.

Anti-apoptotic dependency of T-ALL vary according to their phenotype with immature and early cortical T-ALL survival relying essentially on BCL2.[56] We thus wondered whether *PHF6* alterations could be associated with better response to 5-azacytidine and venetoclax combination, a reference treatment combination for AML uneligible for intensive chemotherapy and an emerging one for T-ALL (43–45). Of note, within GRAALL03/05 cohort, *PHF6*^{ALT} T-ALL indeed displayed higher BCL2 transcript expression when compared to WT, further supporting this rational (Figure 5C). We therefore tested this combination ex vivo, on fresh blasts from the same patients depicted in fig. 5B. There was no significant difference between *PHF6*^{ALT} and WT samples when exposed to 125 nM of venetoclax. Nevertheless, *PHF6*^{ALT} blasts were significantly more sensitive to the combination of both drugs when compared to WT (Figure 5D). Again, PRC2^{ALT} T-ALL displayed similar response profile to this combination.

Given these results, we investigated the efficacy of this combination at relapse in a small cohort of patients with relapsed or refractory disease. Three R/R *PHF6*^{ALT} patients (from those tested in vitro in Figure 5B and D, details are provided in Supplementary Table 3) were treated with 5-azacytidine and venetoclax combination at relapse (Figure 5E). Patient 1 (T-ALL1) presented with T lymphoblastic lymphoma at diagnosis and relapsed as a T-ALL during the first year of treatment according to the standard of care. He received a total of three lines of treatment before benefiting from 5-azacytidine and venetoclax combination. Complete bone marrow blast clearance and metabolic response, assessed by positron emission tomography (PET), was achieved after the first course of treatment. Patient 2 (T-ALL2) was treated with 5-

azacytidine and venetoclax upon mediastinal relapse 15 months after HSCT. Complete morphological and metabolical response (Deauville 4), was obtained after two courses of treatment. Patient 3 (T-ALL3) was treated with the same combination at relapse with cutaneous and CNS involvement, four years after HSCT. Complete medullary and extramedullary response was achieved after two courses and four intrathecal chemotherapies, allowing second HSCT. Apart from expected adverse events, treatment was well tolerated. All three patients are alive at the time of writing this manuscript. Taken together, these results suggest that PHF6 LoF is associated to increased sensitivity to 5-azacytidine alone or in combination with venetoclax.

Discussion

This study is the first to assess *PHF6* alterations incidence and clinical impact in a large protocolar study. Consistent with previous literature, *PHF6* alterations are frequent in GRAALL 2003-2005 cohort (10,20–27). As reported in previous studies, *PHF6* alterations are strongly associated to TLX oncotypes, with particular emphasis for TLX1. PHF6 LoF seems to be mutually exclusive with a mature TCRAB phenotype in T-ALL and with known TAL1 expression deregulations.

We revealed that *PHF6*^{ALT} T-ALL are characterized by high overall DNA methylation. Differentially hypermethylated probes were highly enriched in CGIs located at regions physiologically bearing bivalent H3K4me3 and/or H3K27me3 histone marks. Such chromatin is frequently associated with genes regulated by Polycomb complexes and H3K4me3 depositing proteins such as COMPASS and MLL2 (KMT2B/D) complexes (37,46,47). These genes are involved in developmental processes and thought to display highly variable and finely tuned expression. Moreover, they have been implicated in the regulation of lineage specificity and functional plasticity of differentiating CD4+ T cells, revealing their importance during thymocytes maturation

(48). Many bivalent genes in human ES cells (hESC) are frequent targets for hypermethylation in human cancers and growing evidence suggests a role in carcinogenesis can be find in literature (40,46,49–51). Our results show that thymic bivalent promoters are maintained strictly hypomethylated during thymopoiesis. Even though hypermethylation of these promoters had little impact on bivalent genes expression in PHF6^{ALT} T-ALL, loss of PHF6 and subsequent modification of the epigenetic landscape could participate to leukemogenesis by altering thymopoiesis. Supporting a role for PHF6 in T cell development, mouse models did find altered thymopoiesis with reduced DN2 and DN3 thymocytes, as well as lower counts of T cells in peripheral blood after conditional Phf6 KO (28,30,52).

PRC2 is thought to protect CGIs from methylation, directly or through the recruitment of other epigenetic regulators like TET proteins (41,42,53). DNA hypermethylation of PRC2 target genes have already been described in T-ALL (42,54). Our results indicate that PHF6 and/or PRC2-altered T-ALL display a switch from a labile and permissive silencing of bivalent genes, insured by H3K27me3, to a more static state following DNA hypermethylation (55). We propose that both PHF6 and PRC2 complex are implicated in the maintenance of thymic bivalent regions and might protect them from DNA methylation in a similar manner. Mutual exclusion of PHF6 and DNMT3A LoF suggests that this hypermethylation is crucial during T leukemogenesis. Notably, PHF6 locates at bivalent promoters and has been shown to interact with RBBP4, a member of PRC2, MLL2 and NuRD complexes, all implicated in bivalent promoters maintenance (47,56,57). Moreover, the co-occurrence of *PHF6* and PRC2 alterations support a collaborative interaction during leukemogenesis. Surprisingly, *PHF6*^{ALT}/PRC2^{WT} T-ALL only showed a drastic reduction in H3K27me3 mark at bivalent promoters while *PHF6*^{WT}/PRC2^{ALT} had almost none. These results could be explained by residual

activity of the PRC2 complex due to sufficient expression of the remaining wild type allele in *PHF6*^{WT}/PRC2^{ALT} T-ALL. Because of its location on X chromosome, *PHF6* is more prone to permanent LoF when mutated, even in the case of female patient, as a result of X inactivation. However, both *PHF6*^{ALT}/PRC2^{WT} and *PHF6*^{WT}/PRC2^{ALT} T-ALL display hypermethylation of bivalent promoters suggesting that loss of H3K27me3 is dispensable during this process. Overall, this study supports a model in which PHF6 and PRC2 complex collaborates to maintain bivalent promoters hypomethylated. Functional studies are required to detail the role of PHF6 in maintaining H3K27me3 marks at bivalent promoters and in preventing them from DNA hypermethylation during leukemogenesis.

We demonstrate that *PHF6* alterations are conserved during the clonal evolution of the disease and might provide better clonal fitness at relapse as suggested in previous publications (28,31). It has also been suggested that PHF6 LoF is an early event during leukemogenesis (28). Nevertheless, this event is not sufficient to specifically develop T-ALL, as mice lacking PHF6 develop a heterogeneous spectrum of hemopathies, and further leukemogenic events may be required to develop T-ALL, such as homeodomain protein overexpression (30). The loss of epigenetic plasticity following PHF6 alteration and DNA hypermethylation could participate in early leukemogenesis, by slowing down the differentiation program of thymocytes as it is suggested for other cancer (55). This epigenetic state, and the LoF of PHF6 itself, could lead to genomic instability and appearance of chromosomal rearrangement responsible for ectopic expression of homeobox transcription factor such as TLXs (55,58). Importantly, we showed that TLX1 does not locate at bivalent promoters suggesting that its overexpression may not be directly responsible for the epigenetic changes depicted in this study. The strong association between *PHF6* alterations and homeodomain

oncotypes also supports oncogenic cooperation. However, further studies are needed to explore the role and chronology of *PHF6* LoF in leukemogenesis.

Finally, our results show that *PHF6* alterations are associated with better overall survival, event-free survival, and lower cumulative risk of relapse, independently of other known prognostic parameters. Moreover, despite significantly older age, patient with *PHF6*^{ALT} T-ALL achieve complete remission significantly more often and have lower incidence of death during induction treatment. However, according to this study, one out of four *PHF6*^{ALT} patients still experienced relapsed or refractory disease. Hence, novel treatments are still needed for those patients. PHF6 alterations are largely conserved at relapse and are therefore potential biomarkers for innovative targeted therapies. This study reveals increased in vitro and in vivo sensitivity of *PHF6*^{ALT} T-ALL to the demethylating agent 5-azacytidine alone and in combination with the BCL2 inhibitor venetoclax. Such treatment combination has recently become a standard of care for patients diagnosed with AML and not eligible for intensive chemotherapy induction, and has been given to patients presenting R/R T-ALL (44,45). These observations led us to treat three patients bearing *PHF6* alterations with good response and minimal toxicity. Altogether, this study provides clinical evidence that *PHF6* alterations is associated with 5-azacytidine and venetoclax combination response and might therefore be used as surrogate of eligibility to this treatment.

Acknowledgment

This manuscript was written on behalf of The Group for Research on Adult Acute Lymphoblastic Leukemia (GRAALL), which includes the former France-Belgium Group for Lymphoblastic Acute Leukemia in Adults (LALA), the French Western-Eastern Group for Lymphoblastic Acute Leukemia (GOELAL), and the Swiss Group for Clinical Cancer Research (SAKK). The authors thank all participants in the GRAALL-2003 and

GRAALL-2005 study groups for collection and provision of data and patient samples. The authors also thank Marie-Christine Bene, Mathilde Hunault-Berger, and Etienne Lengline for their constructive revision of the manuscript.

The GRAALL-2003 study was sponsored by the Hôpitaux de Toulouse and the GRAALL-2005 study by the Assistance Publique–Hôpitaux de Paris. The SAKK was supported by the Swiss State Secretariat for Education, Research and Innovation (SERI) Switzerland. The Necker laboratory is supported by the Association “Fédération Leucémie Espoir”, the Association “Force Hémato”, the Association pour la Recherche contre le Cancer (Equipe ARC Labellisée).

References

1. Asnafi V, Beldjord K, Boulanger E, et al. Analysis of TCR, pTα, and RAG-1 in T-acute lymphoblastic leukemias improves understanding of early human T-lymphoid lineage commitment. *Blood*. 2003;101(7):2693-2703. doi:10.1182/blood-2002-08-2438

2. Desjonquères A, Chevallier P, Thomas X, et al. Acute lymphoblastic leukemia relapsing after first-line pediatric-inspired therapy: a retrospective GRAALL study. *Blood Cancer Journal*. 2016;6(12):e504-e504. doi:10.1038/bcj.2016.111

3. Gökbuget N, Kneba M, Raff T, et al. Adult patients with acute lymphoblastic leukemia and molecular failure display a poor prognosis and are candidates for stem cell transplantation and targeted therapies. *Blood*. 2012;120(9):1868-1876. doi:10.1182/blood-2011-09-377713

4. Gökbuget N, Stanze D, Beck J, et al. Outcome of relapsed adult lymphoblastic leukemia depends on response to salvage chemotherapy, prognostic factors, and performance of stem cell transplantation. *Blood*. 2012;120(10):2032-2041. doi:10.1182/blood-2011-12-399287

5. Litzow MR, Ferrando AA. How I treat T-cell acute lymphoblastic leukemia in adults. *Blood*. 2015;126(7):833-841. doi:10.1182/blood-2014-10-551895

6. Van der Meulen J, Van Roy N, Van Vlierberghe P, Speleman F. The epigenetic landscape of T-cell acute lymphoblastic leukemia. *The International Journal of Biochemistry & Cell Biology*. 2014;53:547-557. doi:10.1016/j.biocel.2014.04.015

7. Touzart A, Mayakonda A, Smith C, et al. Epigenetic analysis of patients with T-ALL identifies poor outcomes and a hypomethylating agent-responsive subgroup. *Science Translational Medicine*. 2021;13(595):eabc4834. doi:10.1126/scitranslmed.abc4834

8. Lower KM, Turner G, Kerr BA, et al. Mutations in PHF6 are associated with Börjeson–Forssman –Lehmann syndrome. *Nat Genet*. 2002;32(4):661-665. doi:10.1038/ng1040

9. Todd MAM, Ivanochko D, Picketts DJ. PHF6 Degrees of Separation: The Multifaceted Roles of a Chromatin Adaptor Protein. *Genes*. 2015;6(2):325-352. doi:10.3390/genes6020325

10. Van Vlierberghe P, Palomero T, Khiabanian H, et al. PHF6 mutations in T-cell acute lymphoblastic leukemia. *Nat Genet*. 2010;42(4):338-342. doi:10.1038/ng.542

11. Van Vlierberghe P, Patel J, Abdel-Wahab O, et al. PHF6 mutations in adult acute myeloid leukemia. *Leukemia*. 2011;25(1):130-134. doi:10.1038/leu.2010.247

12. Alexander TB, Gu Z, Iacobucci I, et al. The genetic basis and cell of origin of mixed phenotype acute leukaemia. *Nature*. 2018;562(7727):373-379. doi:10.1038/s41586-018-0436-0

13. Yoshizato T, Dumitriu B, Hosokawa K, et al. Somatic Mutations and Clonal Hematopoiesis in Aplastic Anemia. *New England Journal of Medicine*. 2015;373(1):35-47. doi:10.1056/NEJMoa1414799

14. Bond J, Krzywon A, Lhermitte L, et al. A transcriptomic continuum of differentiation arrest identifies myeloid interface acute leukemias with poor prognosis. *Leukemia*. 2021;35(3):724-736. doi:10.1038/s41375-020-0965-z

15. Zhang C, Mejia LA, Huang J, et al. The X-Linked Intellectual Disability Protein PHF6 Associates with the PAF1 Complex and Regulates Neuronal Migration in the Mammalian Brain. *Neuron*. 2013;78(6):986-993. doi:10.1016/j.neuron.2013.04.021

16. Todd MAM, Huh MS, Picketts DJ. The sub-nucleolar localization of PHF6 defines its role in rDNA transcription and early processing events. *Eur J Hum Genet*. 2016;24(10):1453-1459. doi:10.1038/ejhg.2016.40

17. Wang J, Leung JW chung, Gong Z, Feng L, Shi X, Chen J. PHF6 Regulates Cell Cycle Progression by Suppressing Ribosomal RNA Synthesis *. *Journal of Biological Chemistry*. 2013;288(5):3174-3183. doi:10.1074/jbc.M112.414839

18. Todd MAM, Picketts DJ. PHF6 Interacts with the Nucleosome Remodeling and Deacetylation (NuRD) Complex. *J Proteome Res*. Published online 2012:12.

19. Gursoy-Yuzugullu O, House N, Price BD. Patching Broken DNA: Nucleosome Dynamics and the Repair of DNA Breaks. *Journal of Molecular Biology*. 2016;428(9, Part B):1846-1860. doi:10.1016/j.jmb.2015.11.021

20. Yeh TC, Liang DC, Liu HC, et al. Clinical and biological relevance of genetic alterations in pediatric T-cell acute lymphoblastic leukemia in Taiwan. *Pediatric Blood & Cancer*. 2019;66(1):e27496. doi:10.1002/pbc.27496

21. Spinella JF, Cassart P, Richer C, et al. Genomic characterization of pediatric T-cell acute lymphoblastic leukemia reveals novel recurrent driver mutations. *Oncotarget*. 2016;7(40):65485-65503. doi:10.18632/oncotarget.11796

22. Zhang J, Ding L, Holmfeldt L, et al. The genetic basis of early T-cell precursor acute lymphoblastic leukaemia. *Nature*. 2012;481(7380):157-163. doi:10.1038/nature10725

23. Vicente C, Schwab C, Broux M, et al. Targeted sequencing identifies associations between IL7R-JAK mutations and epigenetic modulators in T-cell acute lymphoblastic leukemia. *Haematologica*. 2015;100(10):1301-1310. doi:10.3324/haematol.2015.130179

24. Teachey DT, Pui CH. Comparative features and outcomes between paediatric T-cell and B-cell acute lymphoblastic leukaemia. *The Lancet Oncology*. 2019;20(3):e142-e154. doi:10.1016/S1470-2045(19)30031-2

25. Chang YH, Yu CH, Jou ST, et al. Targeted sequencing to identify genetic alterations and prognostic markers in pediatric T-cell acute lymphoblastic leukemia. *Sci Rep*. 2021;11(1):769. doi:10.1038/s41598-020-80613-6

26. Wang Q, Qiu H, Jiang H, et al. Mutations of PHF6 are associated with mutations of NOTCH1, JAK1 and rearrangement of SET-NUP214 in T-cell acute lymphoblastic leukemia. *Haematologica*. 2011;96(12):1808-1814. doi:10.3324/haematol.2011.043083

27. Liu Y, Easton J, Shao Y, et al. The genomic landscape of pediatric and young adult T-lineage acute lymphoblastic leukemia. *Nature Genetics*. 2017;49(8):1211-1218. doi:10.1038/ng.3909

28. Wendorff AA, Quinn SA, Rashkovan M, et al. Phf6 Loss Enhances HSC Self-Renewal Driving Tumor Initiation and Leukemia Stem Cell Activity in T-ALL. *Cancer Discov*. 2019;9(3):436-451. doi:10.1158/2159-8290.CD-18-1005

29. Miyagi S, Sroczynska P, Kato Y, et al. The chromatin-binding protein Phf6 restricts the self-renewal of hematopoietic stem cells. *Blood*. 2019;133(23):2495-2506. doi:10.1182/blood.2019000468

30. McRae HM, Garnham AL, Hu Y, et al. PHF6 regulates hematopoietic stem and progenitor cells and its loss synergizes with expression of TLX3 to cause leukemia. *Blood*. 2019;133(16):1729-1741. doi:10.1182/blood-2018-07-860726

31. Yuan S, Wang X, Hou S, et al. PHF6 and JAK3 mutations cooperate to drive T-cell acute lymphoblastic leukemia progression. *Leukemia*. 2022;36(2):370-382. doi:10.1038/s41375-021-01392-1

32. Xiang J, Wang G, Xia T, Chen Z. The depletion of PHF6 decreases the drug sensitivity of T-cell acute lymphoblastic leukemia to prednisolone. *Biomedicine & Pharmacotherapy*. 2019;109:2210-2217. doi:10.1016/j.biopha.2018.11.083

33. Tsai H i, Wu Y, Huang R, et al. PHF6 functions as a tumor suppressor by recruiting methyltransferase SUV39H1 to nucleolar region and offers a novel therapeutic target for PHF6-muntant leukemia. *Acta Pharmaceutica Sinica B*. 2022;12(4):1913-1927. doi:10.1016/j.apsb.2021.10.025

34. Andrieu GP, Kohn M, Simonin M, et al. PRC2 loss of function confers a targetable vulnerability to BET proteins in T-ALL. *Blood*. 2021;138(19):1855-1869. doi:10.1182/blood.2020010081

35. Trinquand A, Tanguy-Schmidt A, Ben Abdelali R, et al. Toward a NOTCH1/FBXW7/RAS/PTEN–Based Oncogenetic Risk Classification of Adult T-Cell Acute Lymphoblastic Leukemia: A Group for Research in Adult Acute Lymphoblastic Leukemia Study. *JCO*. 2013;31(34):4333-4342. doi:10.1200/JCO.2012.48.5292

36. Bernstein BE, Mikkelsen TS, Xie X, et al. A Bivalent Chromatin Structure Marks Key Developmental Genes in Embryonic Stem Cells. *Cell*. 2006;125(2):315-326. doi:10.1016/j.cell.2006.02.041

37. Macrae TA, Fothergill-Robinson J, Ramalho-Santos M. Regulation, functions and transmission of bivalent chromatin during mammalian development. *Nat Rev Mol Cell Biol*. 2023;24(1):6-26. doi:10.1038/s41580-022-00518-2

38. Cieslak A, Charbonnier G, Tesio M, et al. Blueprint of human thymopoiesis reveals molecular mechanisms of stage-specific TCR enhancer activation. *Journal of Experimental Medicine*. 2020;217(9):e20192360. doi:10.1084/jem.20192360

39. Zou Z, Ohta T, Miura F, Oki S. ChIP-Atlas 2021 update: a data-mining suite for exploring epigenomic landscapes by fully integrating ChIP-seq, ATAC-seq and Bisulfite-seq data. *Nucleic Acids Research*. 2022;50(W1):W175-W182. doi:10.1093/nar/gkac199

40. Bernhart SH, Kretzmer H, Holdt LM, et al. Changes of bivalent chromatin coincide with increased expression of developmental genes in cancer. *Sci Rep*. 2016;6(1):37393. doi:10.1038/srep37393

41. Li Y, Zheng H, Wang Q, et al. Genome-wide analyses reveal a role of Polycomb in promoting hypomethylation of DNA methylation valleys. *Genome Biology*. 2018;19(1):18. doi:10.1186/s13059-018-1390-8

42. Mochizuki-Kashio M, Aoyama K, Sashida G, et al. Ezh2 loss in hematopoietic stem cells predisposes mice to develop heterogeneous malignancies in an Ezh1-dependent manner. *Blood*. 2015;126(10):1172-1183. doi:10.1182/blood-2015-03-634428

43. DiNardo CD, Wei AH. How I treat acute myeloid leukemia in the era of new drugs. *Blood*. 2020;135(2):85-96. doi:10.1182/blood.2019001239

44. Wan CL, Zou JY, Qiao M, et al. Venetoclax combined with azacitidine as an effective and safe salvage regimen for relapsed or refractory T-cell acute lymphoblastic leukemia: a case series. *Leukemia & Lymphoma*. 2021;62(13):3300-3303. doi:10.1080/10428194.2021.1957876

45. Farhadfar N, Li Y, May WS, Adams CB. Venetoclax and decitabine for treatment of relapsed T-cell acute lymphoblastic leukemia: A case report and review of literature. *Hematology/Oncology and Stem Cell Therapy*. 2021;14(3):246-251. doi:10.1016/j.hemonc.2019.10.002

46. Blanco E, González-Ramírez M, Alcaine-Colet A, Aranda S, Di Croce L. The Bivalent Genome: Characterization, Structure, and Regulation. *Trends in Genetics*. 2020;36(2):118-131. doi:10.1016/j.tig.2019.11.004

47. Harikumar A, Meshorer E. Chromatin remodeling and bivalent histone modifications in embryonic stem cells. *EMBO reports*. 2015;16(12):1609-1619. doi:10.15252/embr.201541011

48. Wei G, Wei L, Zhu J, et al. Global Mapping of H3K4me3 and H3K27me3 Reveals Specificity and Plasticity in Lineage Fate Determination of Differentiating CD4+ T Cells. *Immunity*. 2009;30(1):155-167. doi:10.1016/j.immuni.2008.12.009

49. Hinoue T, Weisenberger DJ, Lange CPE, et al. Genome-scale analysis of aberrant DNA methylation in colorectal cancer. *Genome Res*. 2012;22(2):271-282. doi:10.1101/gr.117523.110

50. Kumar V, Alt FW, Oksenych V. Functional Overlaps Between XLF and The ATM-dependent DNA Double Strand Break Response. *DNA Repair (Amst)*. 2014;16:11-22. doi:10.1016/j.dnarep.2014.01.010

51. Dunican DS, Mjoseng HK, Duthie L, Flyamer IM, Bickmore WA, Meehan RR. Bivalent promoter hypermethylation in cancer is linked to the H327me3/H3K4me3 ratio in embryonic stem cells. *BMC Biology*. 2020;18(1):25. doi:10.1186/s12915-020-0752-3

52. Hsu YC, Chen TC, Lin CC, et al. Phf6-null hematopoietic stem cells have enhanced self-renewal capacity and oncogenic potentials. *Blood Advances*. 2019;3(15):2355-2367. doi:10.1182/bloodadvances.2019000391

53. Manzo M, Wirz J, Ambrosi C, Villaseñor R, Roschitzki B, Baubec T. Isoform-specific localization of DNMT3A regulates DNA methylation fidelity at bivalent CpG islands. *The EMBO Journal*. 2017;36(23):3421-3434. doi:10.15252/embj.201797038

54. Roels J, Thénoz M, Szarzyńska B, et al. Aging of Preleukemic Thymocytes Drives CpG Island Hypermethylation in T-cell Acute Lymphoblastic Leukemia. *Blood Cancer Discovery*. 2020;1(3):274-289. doi:10.1158/2643-3230.BCD-20-0059

55. Flavahan WA, Gaskell E, Bernstein BE. Epigenetic plasticity and the hallmarks of cancer. *Science*. 2017;357(6348):eaal2380. doi:10.1126/science.aal2380

56. Liu Z, Li F, Zhang B, Li S, Wu J, Shi Y. Structural Basis of Plant Homeodomain Finger 6 (PHF6) Recognition by the Retinoblastoma Binding Protein 4 (RBBP4) Component of the Nucleosome Remodeling and Deacetylase (NuRD) Complex *. *Journal of Biological Chemistry*. 2015;290(10):6630-6638. doi:10.1074/jbc.M114.610196

57. Meacham CE, Lawton LN, Soto-Feliciano YM, et al. A genome-scale in vivo loss-of-function screen identifies Phf6 as a lineage-specific regulator of leukemia cell growth. *Genes Dev*. 2015;29(5):483-488. doi:10.1101/gad.254151.114

58. Alvarez S, da Silva Almeida AC, Albero R, et al. Functional mapping of PHF6 complexes in chromatin remodeling, replication dynamics, and DNA repair. *Blood*. 2022;139(23):3418-3429. doi:10.1182/blood.2021014103

59. Beldjord K, Chevret S, Asnafi V, et al. Oncogenetics and minimal residual disease are independent outcome predictors in adult patients with acute lymphoblastic leukemia. *Blood*. 2014;123(24):3739-3749. doi:10.1182/blood-2014-01-547695

60. Ritchie ME, Phipson B, Wu D, et al. limma powers differential expression analyses for RNA-sequencing and microarray studies. *Nucleic Acids Research*. 2015;43(7):e47. doi:10.1093/nar/gkv007

Tables

Clinical characteristics	All N = 216	PHF6^{ALT} N = 102	PHF6^{WT} N = 114	p
Patients characteristics				
Median age (CI)	30.49 (16.27 - 59.15)	34.17 (16.42 - 58.05)	28.22 (16.27 - 59.15)	0.04
White cell count in G/L (CI)	35.15 (1.00 - 645.00)	33.00 (1.00 - 604.40)	40.45 (2.20 - 645.00)	0.90
CNS involvment (%)	24 (11%)	10 (10%)	14 (12%)	0.67
Treatment response				
Steroid response (%)	117 (54%)	59 (58%)	58 (51%)	0.34
Early BM blast clearance (%)	119 (55%)	56 (55%)	63 (55%)	0.89
Induction mortality rate (%)	9 (4%)	1 (1%)	8 (7%)	0.04
Complete remission rate (%)	199 (92%)	98 (96%)	101 (89%)	0.05
MRD1 < 10^{-4} (%) (N = 122)	38 (31%)	22 (33%)	16 (29%)	0.70
HSCT (%)	77 (36%)	40 (39%)	37 (32%)	0.32
***NOTCH1/FBXW7 - RAS/PTEN* classifier**				
High risk (%)	88 (41%)	28 (27%)	60 (53%)	< 0.001

Outcomes				
Outcome estimations at 5 yrs				
Cumulative incidence of relapse (CI)	0.33 (0.27 - 0.40)	0.27 (0.19 - 0.37)	0.39 (0.30 - 0.49)	0.04
Event-free survival (CI)	0.56 (0.49 - 0.62)	0.63 (0.53 - 0.72)	0.49 (0.40 - 0.58)	0.02
Overall survival (CI)	0.65 (0.58 - 0.71)	0.74 (0.64 - 0.81)	0.57 (0.47 - 0.66)	0.01

Overall survival	**Univariate**			**Multivariate**		
	HR	**CI**	**p**	**HR**	**CI**	**p**
Age	1.03	1.01 - 1.05	0.002	1.05	1.03 - 1.07	<0.001
White cells blood count	1.64	1.11 - 2.40	0.01	1.94	1.29 - 2.91	0.001
CNS involvment	2.43	1.38 - 4.27	0.002	2.27	1.28 - 4.03	0.005
Steroid response	0.62	0.41 - 0.98	0.04	0.92	0.57 - 1.47	0.72
Classifier high risk	2.74	1.75 - 4.29	<0.001	2.48	1.53 - 4.02	<0.001
PHF6^{ALT}	0.51	0.32 - 0.80	0.004	0.58	0.36 - 0.94	0.03

Table 1: Patients clinical characteristics and outcomes.
CI, confidence interval; CNS, central nervous system; HSCT, hematopoietic stem cell transplant; HR, hazard ratio; CI, confidence interval; CNS, central nervous system.

Figure legends

Figure 1: *PHF6* alterations in the GRAALL-2003-2005 studies.

(A) Pie chart indicating the incidence of PHF6 alterations. (B) Pie chart indicating the proportion of the different types of mutations affecting the PHF6 gene in our cohort. (C) Lollipop plots indicating the observed mutations and their consequences. The red bars map the observed chromosomal deletions involving the PHF6 gene in the GRAALL-2003-2005 studies. (D) Oncoplot depicting the genetic anomalies observed in PHF6 WT or altered T-ALL cases of the GRAALL 2003-2005 studies. For each case, their immunophenotype, and ETP classification. As ETP status is separate from the immunophenotypes, some T-ALL cases are both considered as ETP and immature or TCRAB in the analyses. Genes are classified by functional groups. (E) Panel indicating alterations with significantly different frequency between PHF6 WT or altered patients. Statistical differences were compared by Fisher tests. (F) Bar graphs showing the significant association between PHF6 status and the maturation arrest stage. Annotations indicate the incidence of each maturation arrest stage among the entire cohort. PHF6 WT ETP cases are also considered as immature for 16/24, cortical for 4/54, TCRGD for 1/10 and TCRAB for 1/17 cases. For the PHF6 ALT, ETP cases count as immature for 18/28, cortical for 5/53, TCRGD for 1/13. (G) Bar graphs displaying significant association between PHF6 status and the defining T-ALL genetic events.

Figure 2. Clinical impact of *PHF6* alterations in the GRAALL-2003-2005 studies.

(A) Overall survival, (B) event-free survival and (C) cumulative incidence of relapse in the GRAALL 2003-2005 studies. Red curves represent the $PHF6^{ALT}$T-ALL, and blue curves the WT patients.

Figure 3: PHF6ALTT-ALL display highly methylated methylome.

(A) Genome-wide average CpG methylation of PHF6WT and PHF6ALT T-ALL. (B) Number of hyper- and hypomethylated DMPs in PHF6ALTT-ALL. (C and D) Stacked barplots depicting the relative frequency of significant hyper- or hypomethylated CpGs in relation to their CpG location (C) or context (D). (E) Average CpG methylation of hyDMPs of thymocytes, PHF6WT and PHF6ALT T-ALL. (F) Number of hyper- and hypomethylated promoters in PHF6ALT T-ALL. (G) Barplot for the enrichment of hyper- and hypomethylated DMPs in transcription factors target genes and histone marks. Bar color intensity is coded for odds ratio. (H) Heatmap of H3K27me3 (left) and H3K4me3 (right) histone marks peaks at promoters of genes associated to hyDMPs or to random promoters, at different stages of thymopoïesis (ETP = early T precursors, EC = early cortical, LC = late corticals, SP = single positives) Genes are ordered identically for both marks. (I) Genome-wide average CpG methylation of PHF6WT/PRC2WT, PHF6ALT/PRC2WT, PRC2ALT/PHF6WT, PHF6ALT/PRC2ALT T-ALL. (J) Venn diagram of hyDMPs between PHF6ALT/PRC2WT, PRC2ALT/PHF6WT, PHF6ALT/PRC2ALT T-ALL versus None T-ALL. (K) Uniform Manifold Approximation and Projection of samples according to genome-wide methylation levels (β-values). Each dot represent a patient sample and is colored according to PHF6/PRC2 mutational status. (L) Dot plot for the enrichment of hyper-DMPs common or unique to PHF6ALT/PRC2WT, PRC2ALT/PHF6WT, PHF6ALT/PRC2ALT versus PHF6WT/PRC2WT T-ALLs, in transcription factors target genes, histone marks and gene ontology. Dots are sized-coded for adjusted p-values in the -log10 scale, and color intensity is scaled according to odds ratio.

Figure 4: PHF6ALT T-ALL display altered epigenetics landscape of bivalent promoters

(A) Dot plot for the enrichment of TLX1 (HPB-ALL), PHF6 and TAL1 (Jurkat) peaks along with hyDMPs in active or bivalent promoters (x axis) at specific stages of thymopoiesis. Circles are color-coded for significance, dots color gradient represent odds ratio and the size of the dots represents P values in the log10 scale. (B) Heatmap representing the hierarchical clustering of T-ALL samples and normal thymocytes (x-axis) according to the 10 000 most variable CpG β-values associated to active (left) and bivalent (right) promoters (y-axis). (C) Uniform Manifold Approximation and Projection of T-ALL samples and normal thymocytes according to β-values of CpG associated to thymic bivalent promoters. Each dot represent a sample and is colored according to PHF6/PRC2 mutational status. (D) Heatmap of H3K27me3 (top) and H3K4me3 (bottom) histone marks peaks at thymic bivalent promoters in PHF6WT/PRC2WT (lightblue), PHF6ALT/PRC2WT (red), PHF6WT/PRC2ALT (yellow), PHF6ALT/PRC2ALT (black) T-ALL. (E) Venn diagram representing the proportion of thymic bivalent genes associated to hyDMPs. (F) Volcano plot of differentially expressed genes in PHF6ALT versus PHF6WT. Gene list with an absolute log fold change value superior to 2.

Figure 5: 5-azacytidine and venetoclax sensitivity of PHF6^{ALT}T-ALL

(A) Survival for PDX mouse models of primary T-ALL : PHF6^{WT} (UPNT-M894 : Untreated N = 5, Azacitidine N = 3 ; UPNT-M894 : Untreated N = 5, Azacitidine N = 4) and PHF6^{ALT} ((UPNT-M640 : Untreated N = 4, Azacitidine N = 4 ; UPNT-M149 : Untreated N = 5, Azacitidine N = 5)). When blasts count reached 1% in blood, mice were administered with NaCl (Untreated : orange line) or treated with 5-azacytidine in a curative-like manner for 2 weeks (5 mg/kg per day for 5 days a week) (5-azacytidine

in a curative-like manner : green line). P values are calculated by comparing the untreated group with treated group using log-rank test. (B) Viability of T-ALL fresh samples blasts measured after 3 days of treatment with 5-azacytidine at the indicated doses. Means and SEM are plotted (C) BCL2 gene expression levels in $PHF6^{WT}/PRC2^{WT}$ (lightblue), $PHF6^{ALT}/PRC2^{WT}$ (red), $PHF6^{WT}/PRC2^{ALT}$ (yellow), $PHF6^{ALT}/PRC2^{ALT}$ (black) T-ALL (D) Viability of T-ALL fresh samples blasts measured after 3 days of treatment with 5-azacytidine at the indicated doses combined with 125 µM of Venetoclax. Means and SEM are plotted. (E) Clinical timelines of three patient diagnosed with R/R T-ALL treated with 5-Azacytidine and Venetoclax. Timelines are centered on the time of initiation of the combination.

Figure 1

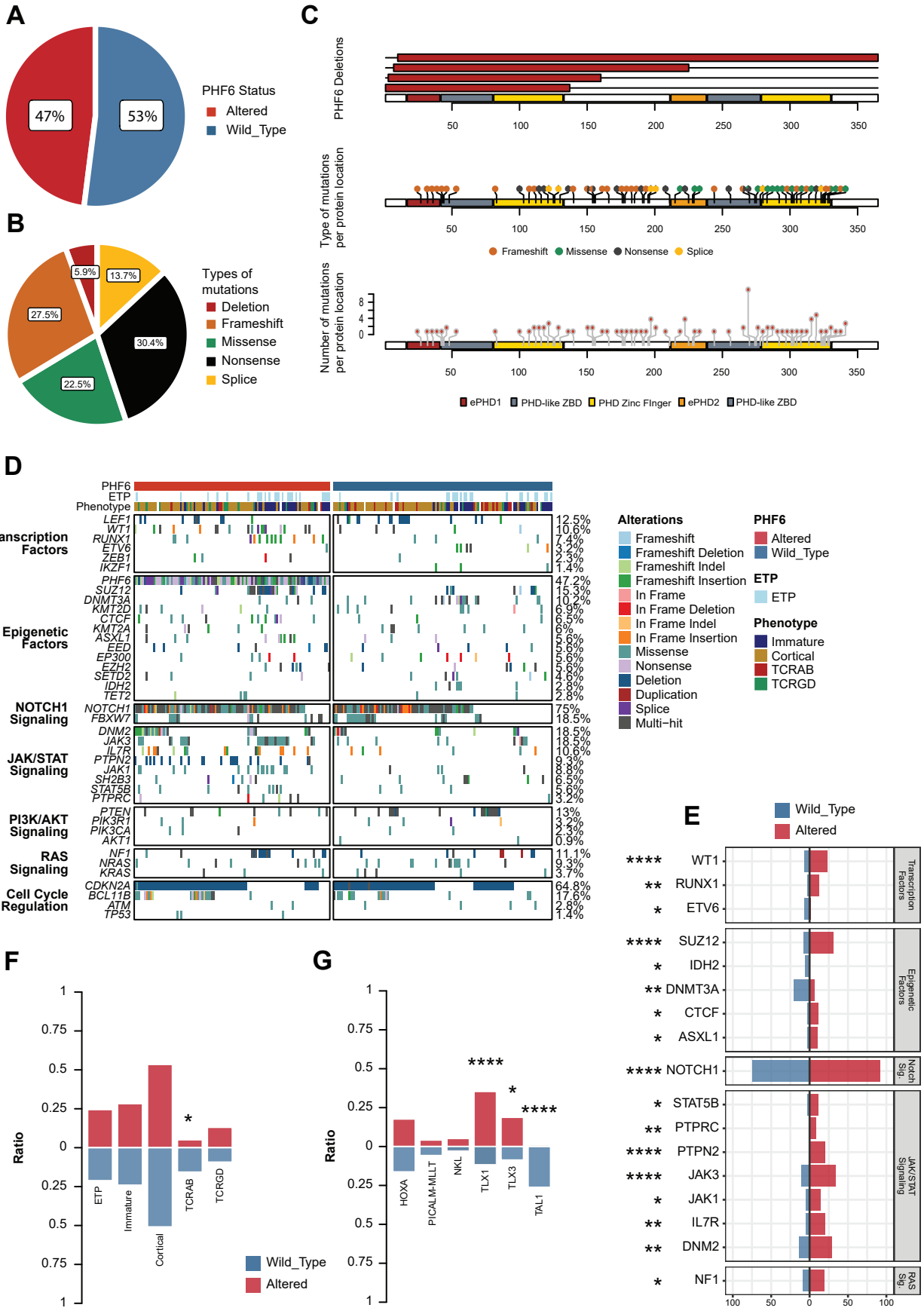
A
47%
53%
PHF6 Status
Altered
Wild_Type
B
5.9%
13.7%
27.5%
30.4%
22.5%
Types of mutations
Deletion
Frameshift
Missense
Nonsense
Splice
C
PHF6 Deletions
Type of mutations per protein location
Frameshift
Missense
Nonsense
Splice
Number of mutations per protein location
ePHD1
PHD-like ZBD
PHD Zinc FInger
ePHD2
PHD-like ZBD
D
PHF6
ETP
Phenotype
Transcription Factors
Epigenetic Factors
NOTCH1 Signaling
JAK/STAT Signaling
PI3K/AKT Signaling
RAS Signaling
Cell Cycle Regulation
Alterations
Frameshift
Frameshift Deletion
Frameshift Indel
Frameshift Insertion
In Frame
In Frame Deletion
In Frame Indel
In Frame Insertion
Missense
Nonsense
Deletion
Duplication
Splice
Multi−hit
PHF6
Altered
Wild_Type
ETP
ETP
Phenotype
Immature
Cortical
TCRAB
TCRGD
E
Wild_Type
Altered
F
Ratio
ETP
Immature
Cortical
TCRAB
TCRGD
Wild_Type
Altered
G
Ratio
HOXA
PICALM-MLLT
NKL
TLX1
TLX3
TAL1

Figure 2

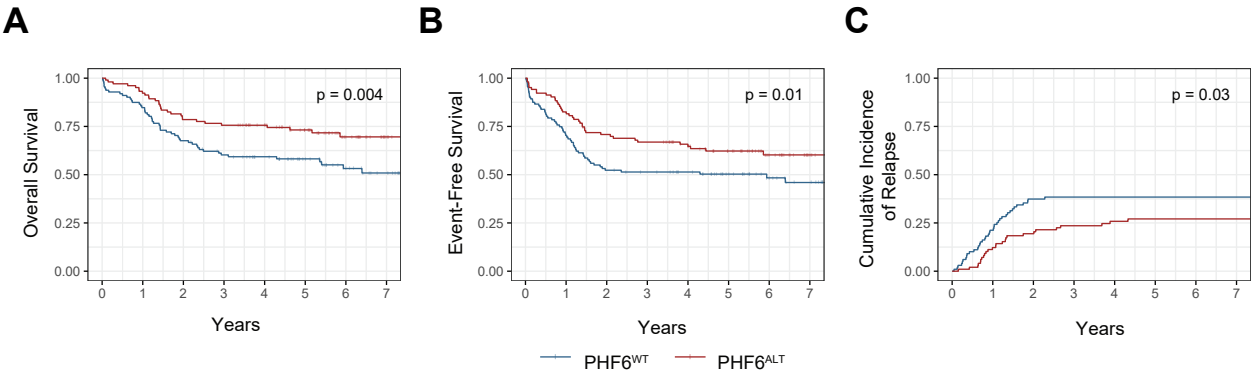
A
B
C
Overall Survival
Event-Free Survival
Cumulative Incidence of Relapse
p = 0.004
p = 0.01
p = 0.03
1.00
0.75
0.50
0.25
0.00
0
1
2
3
4
5
6
7
Years
PHF6WT
PHF6ALT

Figure 3

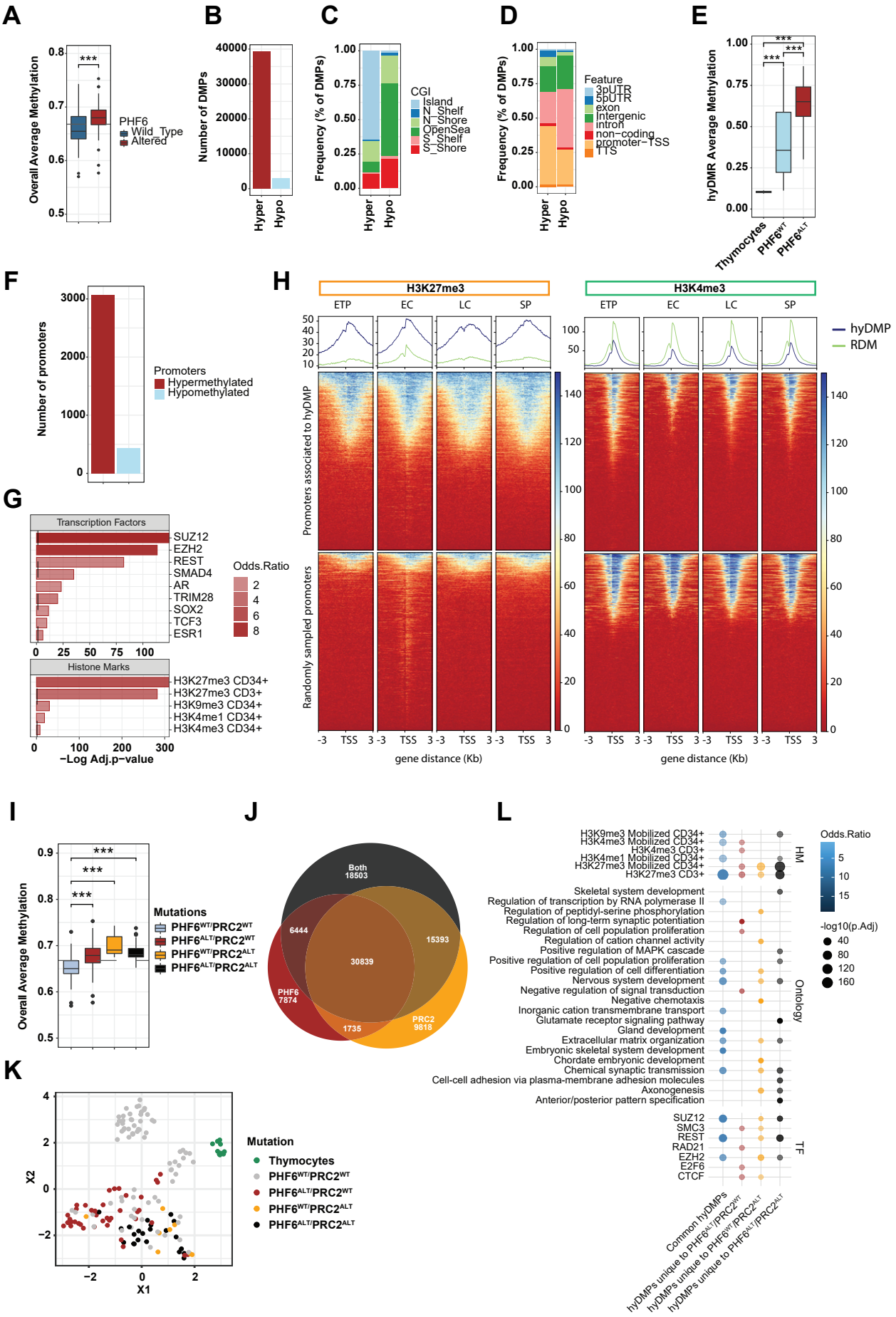
A
Overall Average Methylation
PHF6
Wild_Type
Altered
B
Number of DMPs
Hyper
Hypo
C
Frequency (% of DMPs)
CGI
Island
N_Shelf
N_Shore
OpenSea
S_Shelf
S_Shore
D
Frequency (% of DMPs)
Feature
3pUTR
5pUTR
exon
intergenic
intron
non−coding
promoter−TSS
TTS
E
hyDMR Average Methylation
Thymocytes
PHF6WT
PHF6ALT
F
Number of promoters
Promoters
Hypermethylated
Hypomethylated
G
Transcription Factors
SUZ12
EZH2
REST
SMAD4
AR
TRIM28
SOX2
TCF3
ESR1
Odds.Ratio
Histone Marks
H3K27me3 CD34+
H3K27me3 CD3+
H3K9me3 CD34+
H3K4me1 CD34+
H3K4me3 CD34+
−Log Adj.p−value
H
H3K27me3
H3K4me3
ETP
EC
LC
SP
hyDMP
RDM
Promoters associated to hyDMP
Randomly sampled promoters
TSS
gene distance (Kb)
I
Overall Average Methylation
Mutations
PHF6WT/PRC2WT
PHF6ALT/PRC2WT
PHF6WT/PRC2ALT
PHF6ALT/PRC2ALT
J
Both
18503
6444
15393
30839
PHF6
7874
1735
PRC2
9818
K
X1
X2
Mutation
Thymocytes
PHF6WT/PRC2WT
PHF6ALT/PRC2WT
PHF6WT/PRC2ALT
PHF6ALT/PRC2ALT
L
H3K9me3 Mobilized CD34+
H3K4me3 Mobilized CD34+
H3K4me3 CD3+
H3K4me1 Mobilized CD34+
H3K27me3 Mobilized CD34+
H3K27me3 CD3+
HM
Skeletal system development
Regulation of transcription by RNA polymerase II
Regulation of peptidyl−serine phosphorylation
Regulation of long−term synaptic potentiation
Regulation of cell population proliferation
Regulation of cation channel activity
Positive regulation of MAPK cascade
Positive regulation of cell population proliferation
Positive regulation of cell differentiation
Nervous system development
Negative regulation of signal transduction
Negative chemotaxis
Inorganic cation transmembrane transport
Glutamate receptor signaling pathway
Gland development
Extracellular matrix organization
Embryonic skeletal system development
Chordate embryonic development
Chemical synaptic transmission
Cell−cell adhesion via plasma−membrane adhesion molecules
Axonogenesis
Anterior/posterior pattern specification
Ontology
SUZ12
SMC3
REST
RAD21
EZH2
E2F6
CTCF
TF
Odds.Ratio
-log10(p.Adj)
Common hyDMPs
hyDMPs unique to PHF6ALT/PRC2WT
hyDMPs unique to PHF6WT/PRC2ALT
hyDMPs unique to PHF6ALT/PRC2ALT

Figure 4

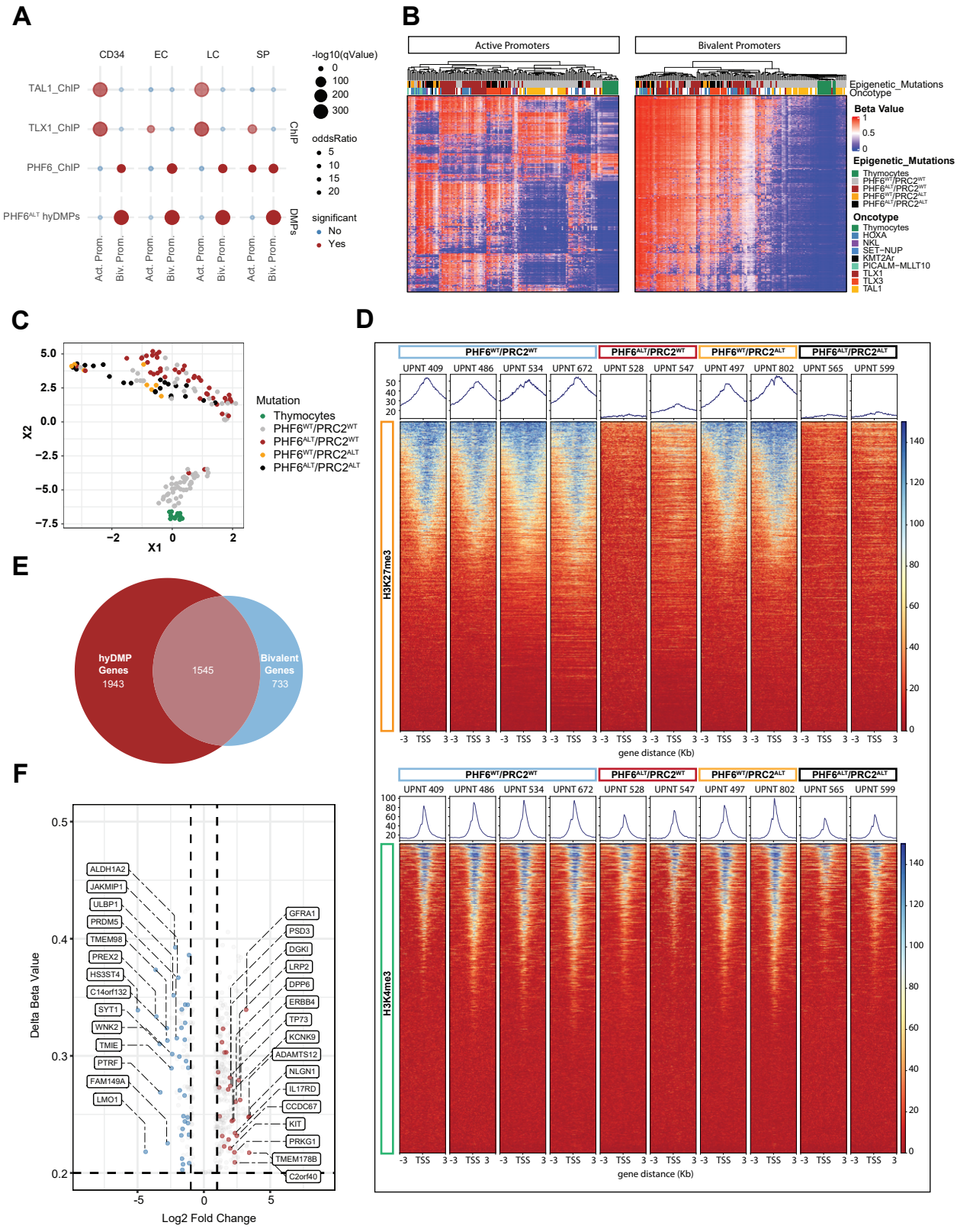
A
CD34
EC
LC
SP
TAL1_ChIP
TLX1_ChIP
PHF6_ChIP
PHF6ALT hyDMPs
ChIP
DMPs
Act. Prom.
Biv. Prom.
-log10(qValue)
0
100
200
300
oddsRatio
5
10
15
20
significant
No
Yes
B
Active Promoters
Bivalent Promoters
Epigenetic_Mutations
Oncotype
Beta Value
1
0.5
0
Epigenetic_Mutations
Thymocytes
PHF6WT/PRC2WT
PHF6ALT/PRC2WT
PHF6WT/PRC2ALT
PHF6ALT/PRC2ALT
Oncotype
Thymocytes
HOXA
NKL
SET-NUP
KMT2Ar
PICALM-MLLT10
TLX1
TLX3
TAL1
C
X2
X1
Mutation
Thymocytes
PHF6WT/PRC2WT
PHF6ALT/PRC2WT
PHF6WT/PRC2ALT
PHF6ALT/PRC2ALT
D
PHF6WT/PRC2WT
PHF6ALT/PRC2WT
PHF6WT/PRC2ALT
PHF6ALT/PRC2ALT
UPNT 409
UPNT 486
UPNT 534
UPNT 672
UPNT 528
UPNT 547
UPNT 497
UPNT 802
UPNT 565
UPNT 599
H3K27me3
H3K4me3
TSS
gene distance (Kb)
E
hyDMP Genes
1943
1545
Bivalent Genes
733
F
Delta Beta Value
Log2 Fold Change
ALDH1A2
JAKMIP1
ULBP1
PRDM5
TMEM98
PREX2
HS3ST4
C14orf132
SYT1
WNK2
TMIE
PTRF
FAM149A
LMO1
GFRA1
PSD3
DGKI
LRP2
DPP6
ERBB4
TP73
KCNK9
ADAMTS12
NLGN1
IL17RD
CCDC67
KIT
PRKG1
TMEM178B
C2orf40

Figure 5

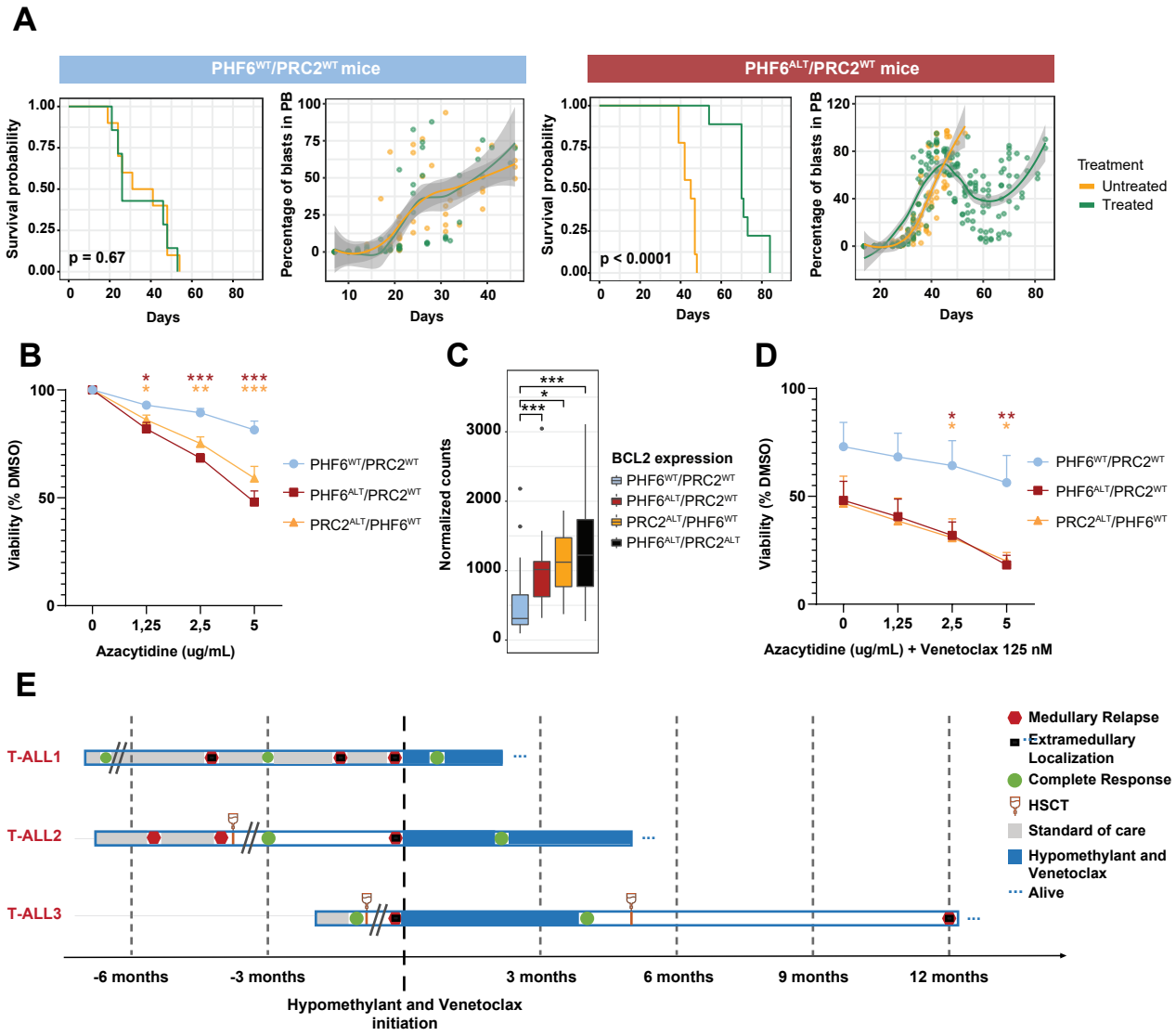
A
PHF6WT/PRC2WT mice
PHF6ALT/PRC2WT mice
Survival probability
p = 0.67
Days
Percentage of blasts in PB
p < 0.0001
Treatment
Untreated
Treated
B
Viability (% DMSO)
Azacytidine (ug/mL)
PHF6WT/PRC2WT
PHF6ALT/PRC2WT
PRC2ALT/PHF6WT
C
Normalized counts
BCL2 expression
PHF6WT/PRC2WT
PHF6ALT/PRC2WT
PRC2ALT/PHF6WT
PHF6ALT/PRC2ALT
D
Viability (% DMSO)
Azacytidine (ug/mL) + Venetoclax 125 nM
E
T-ALL1
T-ALL2
T-ALL3
-6 months
-3 months
3 months
6 months
9 months
12 months
Hypomethylant and Venetoclax initiation
Medullary Relapse
Extramedullary Localization
Complete Response
HSCT
Standard of care
Hypomethylant and Venetoclax
Alive